Supporting Information

Integration of Continuous Microfluidic Electrokinetic Bioparticle Preconcentration with Programmable Extraction into a Discrete Microfluidic Platform

Amir Hillman[1], Sinwook Park[1], Gilad Yossifon[1,2]

[1]School of Mechanical Engineering, Tel-Aviv University, Israel

[2]School of Biomedical Engineering, Tel-Aviv University, Israel

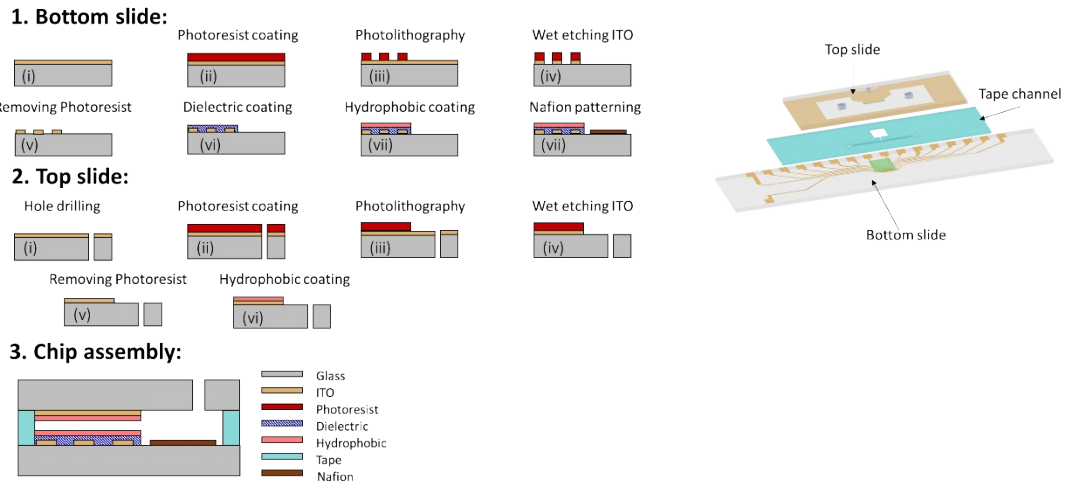

Fig. S1: Fabrication process of the hybrid microchannel-EWOD platform.

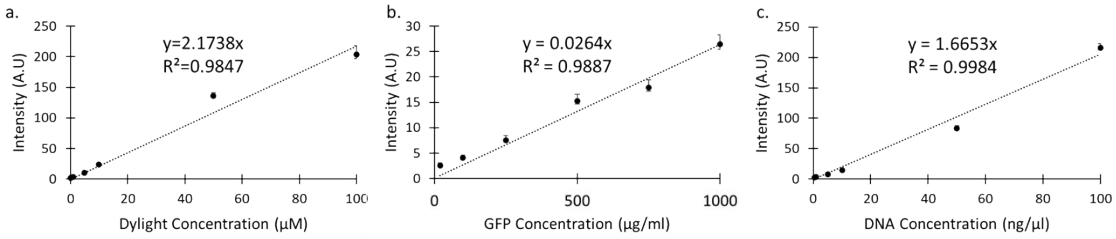

Fig. S2: Calibration of measured fluorescence intensity versus molecule concentration of (a) Dylight, (b) GFP, (c) DNA.

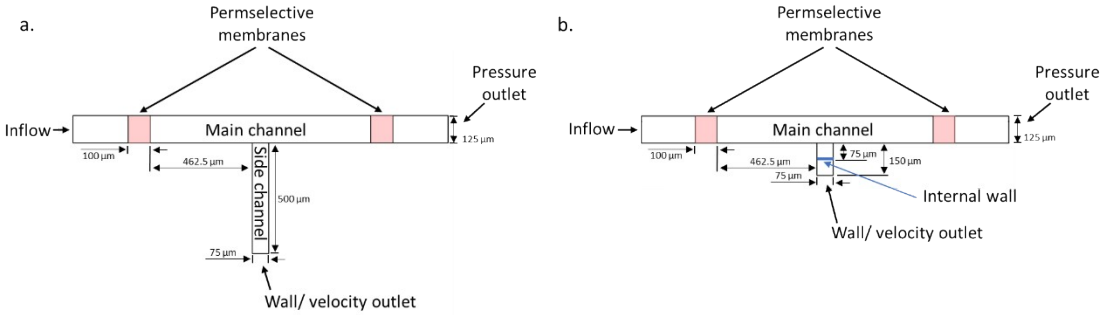

Fig. S3: The geometry of the numerical simulations: (a) The simulation presented in Fig.2b and Fig.3c. The side channel's end is defined as a wall in Fig.2b, and as a velocity outlet in Fig.3c. (b) The geometry of the numerical simulation presented in Fig.4b.

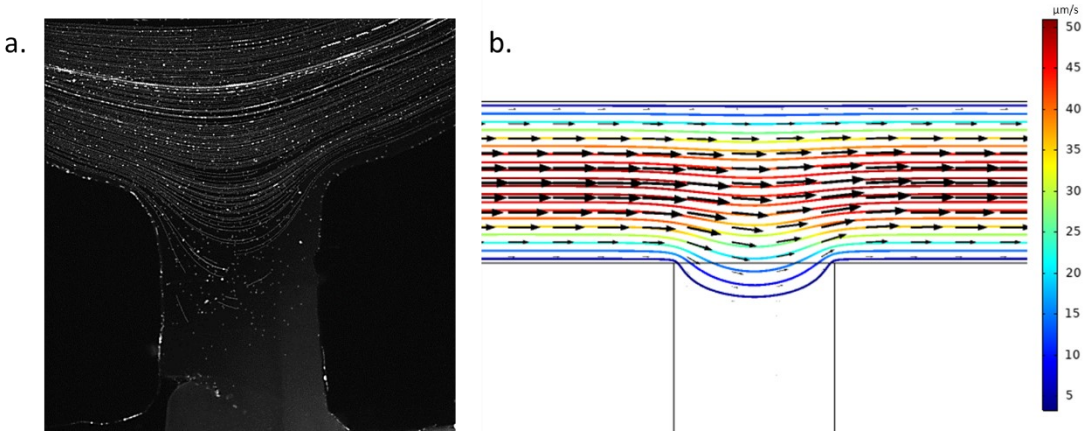

Fig. S4: (a) Experimental and (b) numerical streamlines for the velocity of 50 µm/s. The Experiments were performed using fluorescent polystyrene 1µm as tracers.

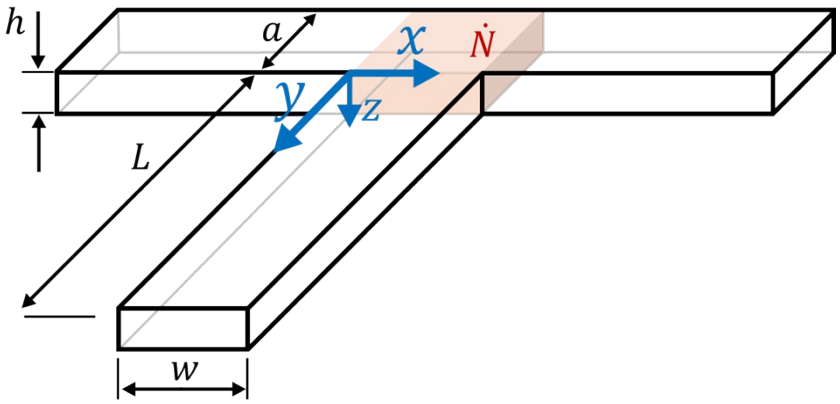

Fig. S5: The geometry of the analytical solution presented in Fig.2c,iii.

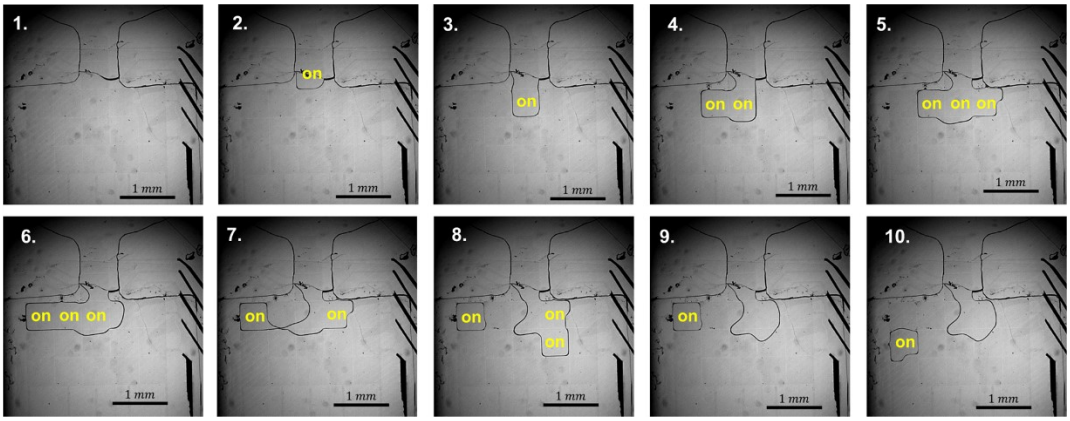

Fig. S6: Time sequences showing the generation of a droplet from the stagnant side channel connecting the EWOD electrodes with the continuous main microchannel.

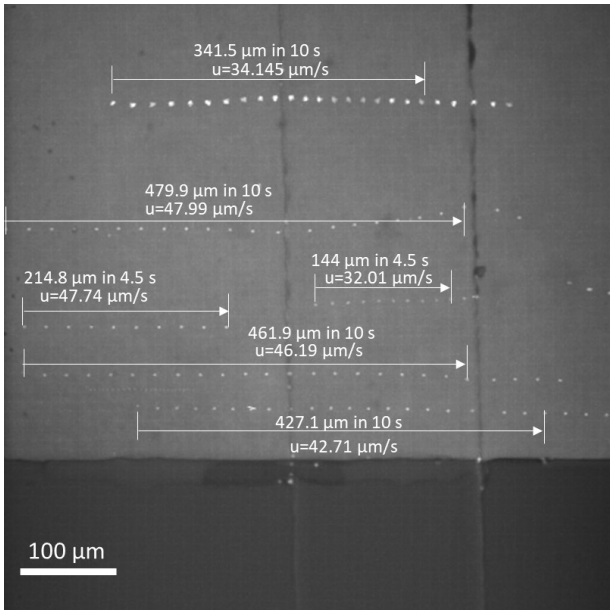

Fig. S7: Flow velocity measurement prior to performing pre-concentration using particle tracking. The measurements considered the horizontal velocity component only.

Analytical model formulation and derivation:

Following the formulation already described in the Materials and Methods section in the manuscript we reformulate Equation 4 in terms of $\breve{C} = C - C_0$ divided into the two regions

$$\frac{\partial \breve{C}_1}{\partial \tau} = \frac{\partial^2 \breve{C}_1}{\partial \eta^2} + \tilde{g},\ 0 < \eta < \tilde{a},\ \tau > 0\ ;\ \breve{C}_1(\eta,0) = 0 \quad , \tag{S1}$$

$$\frac{\partial \breve{C}_2}{\partial \tau} = \frac{\partial^2 \breve{C}_2}{\partial \eta^2},\ \tilde{a} < \eta < 1,\ \tau > 0\ ;\ \breve{C}_2(\eta,0) = 0 \quad , \tag{S2}$$

along with continuity conditions between the regions

$$\tilde{C}_1(\tilde{a},\tau) = \tilde{C}_2(\tilde{a},\tau);\quad \frac{\partial \tilde{C}_1}{\partial \eta}(\tilde{a},\tau) = \frac{\partial \tilde{C}_2}{\partial \eta}(\tilde{a},\tau), \tag{S3}$$

boundary conditions

$$\frac{\partial C_1}{\partial \eta}(0,\tau) = 0;\quad \frac{\partial C_2}{\partial \eta}(1,\tau) = 0\,, \tag{S4}$$

and initial conditions

$$\tilde{C}_1(\eta,0) = \tilde{C}_2(\eta,0) = 0. \tag{S5}$$

The suggested solution is a superposition between a time-dependent homogeneous solution and a time dependent source function

$$\tilde{C}_1(\eta,\tau) = \tilde{C}^*(\eta,\tau) + f_1(\eta,\tau), \tag{S6}$$

$$\tilde{C}_2(\eta,\tau) = \tilde{C}^*(\eta,\tau) + f_2(\eta,\tau). \tag{S7}$$

The suggested homogeneous solution

$$\tilde{C}^*(\eta,\tau) = \sum_{n=0}^{\infty} A_n e^{-(n\pi)^2\tau}\cos(n\pi\eta), \tag{S8}$$

with boundary conditions

$$\left.\frac{\partial \tilde{C}^*}{\partial \eta}\right|_{\eta=0} = \left.\frac{\partial \tilde{C}^*}{\partial \eta}\right|_{\eta=1} = 0, \tag{S9}$$

and initial condition

$$\tilde{C}^*(\eta,0) = 0. \tag{S10}$$

The suggested time-dependent source functions

$$f_1(\eta,\tau) = k\tilde{g}\tau + \frac{1}{2}\tilde{g}(k-1)\eta^2,\ k = const;\ 0 < \eta < \tilde{a}, \tag{S11}$$

$$f_2(\eta,\tau) = k\tilde{g}\tau + \frac{1}{2}k\tilde{g}(\eta-1)^2 + \tilde{g}\beta,\ \beta = const\,;\tilde{a} < \eta < 1. \tag{S12}$$

Hence, the suggested superposition solution for the source included region

$$\tilde{C}_1(\eta,\tau) = \tilde{C}^*(\eta,\tau) + k\tilde{g}\tau + \frac{1}{2}\tilde{g}(k-1)\eta^2,\ k = const;\ 0 < \eta < \tilde{a}. \tag{S13}$$

The suggested superposition solution for the source-free region is

$$\tilde{C}_2(\eta,\tau) = \tilde{C}^*(\eta,\tau) + k\tilde{g}\tau + \frac{1}{2}k\tilde{g}(\eta-1)^2 + \tilde{g}\beta,\ \beta = const\,;\tilde{a} < \eta < 1. \tag{S14}$$

Applying the continuity conditions results in

$$\left.\frac{\partial \tilde{C}^*}{\partial \eta}\right|_{\eta=\tilde{a}} + \tilde{g}(k-1)\tilde{a} = \left.\frac{\partial \tilde{C}^*}{\partial \eta}\right|_{\eta=\tilde{a}} + k\tilde{g}(\tilde{a}-1) \Longrightarrow k = \tilde{a}, \tag{S15}$$

$$\tilde{C}^*(\tilde{a},\tau) + k\tilde{g}\tau + \frac{1}{2}\tilde{g}(k-1)\tilde{a}^2 = \tilde{C}^*(\tilde{a},\tau) + k\tilde{g}\tau + \frac{1}{2}k\tilde{g}(\tilde{a}-1)^2 + \tilde{g}\beta \Longrightarrow \beta = \frac{\tilde{a}}{2}(\tilde{a}-1). \tag{S16}$$

Applying the initial condition to find the coefficients A_n

$$\sum_{n=1}^{\infty} A_n \cos(n\pi\eta) + \frac{1}{2}\tilde{g}(\tilde{a}-1)\eta^2 = 0,\ 0 < \eta < \tilde{a} \quad , \tag{S17}$$

$$\sum_{n=1}^{\infty} A_n \cos(n\pi\eta) + \frac{1}{2}\tilde{g}\left[k(\eta-1)^2 + \tilde{a}(\tilde{a}-1)\right] = 0,\ \tilde{a} < \eta < 1 \quad . \tag{S18}$$

Defining $\tilde{A}_n = \frac{A_n}{\tilde{g}}$. We multiply both sides of the equations by $\cos(m\pi\eta)$ and integrate over the corresponding region. Then by adding (S17) to (S18) we get

$$\int_0^1 \tilde{A}_n \cos(n\pi\eta)\cos(m\pi\eta)d\eta = -\frac{1}{2}\left\{(\tilde{a}-1)\int_0^{\tilde{a}} \eta^2 \cos(m\pi\eta)d\eta + \int_{\tilde{a}}^1 \left[\tilde{a}(\eta-1)^2 + \tilde{a}(\tilde{a}-1)\right]\cos(m\pi\eta)d\eta\right\}, \tag{S19}$$

where for m=n the integrals' solutions

$$\int_0^1 \cos^2(m\pi\eta)d\eta = \frac{2m\pi + \sin(2m\pi)}{4m\pi} \quad , \tag{S20}$$

$$\int_0^{\tilde{a}} \eta^2 \cos(m\pi\eta)d\eta = \frac{(\pi^2\tilde{a}^2m^2 - 2)\sin(m\pi\tilde{a}) + 2\pi\cos(m\pi\tilde{a})\tilde{a}m}{m^3\pi^3} \quad , \tag{S21}$$

$$\int_{\tilde{a}}^1 (\eta-1)^2 \cos(m\pi\eta)d\eta = \frac{\left(2 - m^2(\tilde{a}-1)^2\pi^2\right)\sin(m\pi\tilde{a}) - 2m\pi(\tilde{a}-1)\cos(m\pi\tilde{a}) - 2\sin(m\pi)}{m^3\pi^3} \quad , \tag{S22}$$

$$\int_{\tilde{a}}^1 \cos(m\pi\eta)d\eta = -\frac{\sin(m\pi\tilde{a}) + \sin(m\pi)}{m\pi} \quad . \tag{S23}$$

Hence, the coefficients are defined

$$\tilde{A}_m = -\frac{2\left(2\sin(m\pi\tilde{a}) + \left(-2 + m^2(\tilde{a}-1)\pi^2\right)\sin(m\pi)\tilde{a}\right)}{m^2\pi^2(\cos(m\pi)\sin(m\pi) + m\pi)} \quad . \tag{S24}$$

Adding the zero term for $n = 0$, $\tilde{A}_0$. We apply the initial condition, then multiplying the equation by $\cos(n\pi\eta)$ with $n = 0$, integrating over the corresponding regions and summing between the two regions

$$\int_0^1 \tilde{A}_0 d\eta = -\frac{1}{2}\left\{(\tilde{a}-1)\int_0^{\tilde{a}} \eta^2 d\eta + \int_{\tilde{a}}^1 \left[\tilde{a}(\eta-1)^2 + \tilde{a}(\tilde{a}-1)\right] d\eta\right\}. \quad \text{(S25)}$$

Hence

$$\tilde{A}_0 = \frac{1}{6}\tilde{a}(1-\tilde{a})(2-\tilde{a}). \quad \text{(S26)}$$

Thus, the full solution

$$C(\eta,\tau) = C_0 + A_0 + \sum_{n=1}^{\infty} A_n e^{-(n\pi)^2\tau}\cos(n\pi\eta) + \begin{cases} \tilde{g}\left[\tilde{a}\tau + \frac{1}{2}(\tilde{a}-1)\eta^2\right], & 0 < y < \tilde{a} \\ \tilde{g}\left[\tilde{a}\tau + \frac{1}{2}\tilde{a}(\eta-1)^2 + \frac{\tilde{a}}{2}(\tilde{a}-1), & \tilde{a} < y < 1\right] \end{cases}. \quad \text{(S27)}$$

The solution was plotted in Fig.2.c,iii for the following values, similar to the experiment presented in Fig.2,a:

variable	**value**
a	600 μm
L	1.6 mm
D	3×10^{-10}
c_0	0.001 mol/m^3
w	600 μm
u	42 μm/s

For testing the convergence of the series, the condition where $\tilde{C}_1(0,0) = \tilde{C}_2(1,0)$ are applied

$$\tilde{A}_0 + \sum_{n=1}^{\infty} \tilde{A}_n = \tilde{A}_0 + \sum_{n=1}^{\infty} \tilde{A}_n(-1)^n + \frac{\tilde{a}}{2}(\tilde{a}-1), \quad \text{(S28)}$$

$$\sum_{n=1}^{\infty} \tilde{A}_n - \sum_{n=1}^{\infty} \tilde{A}_n(-1)^n = \frac{\tilde{a}}{2}(\tilde{a}-1). \quad \text{(S29)}$$

Hence for the even sum elements

$$\sum_{m=1}^{\infty} \tilde{A}_{2m} = 0, \quad \text{(S30)}$$

and for the odd sum elements

$$\sum_{m=1}^{\infty} \tilde{A}_{2m-1} = \frac{\tilde{a}}{4}(\tilde{a}-1). \quad \text{(S31)}$$

Hence, calculating the convergence error for different numbers of odd sum elements

$$S(N) = \sum_{m=1}^{N} \tilde{A}_{2m-1} - \frac{\tilde{a}}{4}(\tilde{a}-1). \quad \text{(S32)}$$

Plotting the error as a function of the number of odd elements shows in Fig.S8 that the error S fluctuates around 0, and from the 5th odd element it is converging to 0. Hence, the solution converges after n=10.

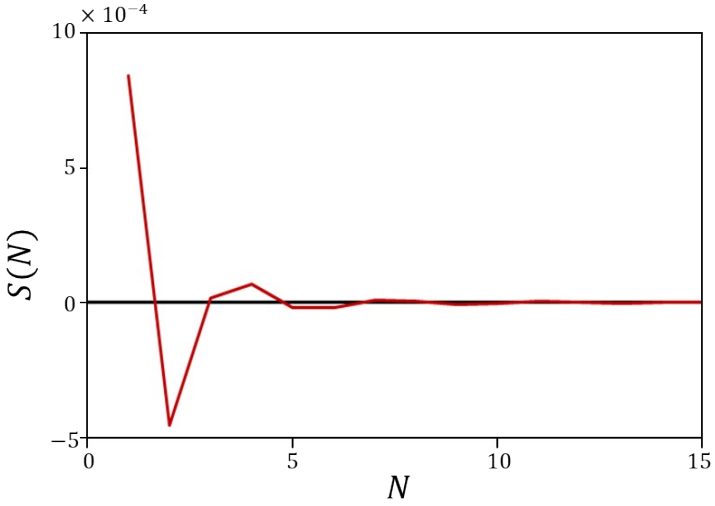

Fig. S8: Convergence test for the analytical solution.

Video S1: Experimental visualization of a preconcentrated fluorescent molecule plug generated via ion concentration polarization within the horizontal microfluidic channel, along with its simultaneous diffusion into the stagnant side channel**.**

Video S2: Numerical simulation of the formation of a preconcentrated molecular plug via ion concentration polarization and its diffusion into the side channel.

Video S3: The generation of three concentrated droplets via electrowetting-on-dielectric**.**

Video S4: Numerical simulation of the convective pulling of the ICP plug into the side channel following its diffusion.

Video S5: Experimental visualization of droplet generation, in which the ICP-preconcentrated plug of fluorescent molecules is transported into the side channel through convective pulling.

Video S6: Numerical simulation of the convective transport of the ICP-preconcentrated plug into the side channel, demonstrating the absence of diffusion during the process**.**

Video S7: Experimental visualization of a DNA concentrated droplet, in which the ICP-preconcentrated plug of DNA molecules is transported into the side channel through convective pulling.

Video S8: Experimental visualization of a GFP concentrated droplet, in which the ICP-preconcentrated plug of GFP molecules is transported into the side channel through convective pulling.